

Accuracy of Specular Path Estimates with ESPRIT and RiMAX in the Presence of Measurement-based Diffuse Multipath Components

Davy P. Gaillot^{*}, Emmeric Tanghe⁺, Paul Stefanut^{*}, Wout Joseph⁺, Martine Lienard^{*}, Pierre Degauque^{*} and Luc Martens⁺

^{*} *University of Lille, IEMN, Group TELICE, Bldg. P3
F 59655 Villeneuve d'Ascq, France
davy.gaillot@univ-lille.fr*

⁺ *Ghent University / IBBT, Dept. of Information Technology, Gaston Crommenlaan 8 box 201
B-9050 Ghent, Belgium
emmeric.tanghe@intec.ugent.be*

Abstract— this paper presents performance results of three high-resolution parameters estimation algorithms: ESPRIT, SAGE and RiMAX. MIMO indoor radio channels which include measurement-based time-delay diffuse multipath scattering (DMC) were emulated to evaluate the estimation performance of both algorithms. The impact of the DMC on the parameter estimation accuracy is studied by adjusting its power with respect to the specular component. For all discussed scenarios, it is clearly demonstrated that RiMAX outperforms ESPRIT and SAGE which do not include DMC estimation into their data model. The preliminary results clearly highlight the importance of DMC and the necessity to account for its presence in data models to accurately estimate the channel parameters. Otherwise, very poor estimates of the coherent component parameters are expected which would in turn result in wronged propagation prediction models.

I. INTRODUCTION

Beyond 3G and 4G mobile radio systems exploit the multipath phenomenon to increase capacity, coverage and quality of service by deploying multiple smart antennas at both the transmitter (Tx) and receiver (Rx) [1]. Consequently, to properly optimize the planning and performance of those future Multiple-In Multiple-Out (MIMO) radio networks, the behaviour of the multi-link double directional propagation channels must be known with sufficient details. This task is particularly challenging in confined environments where the propagating radio waves suffer complex superimposed reflection, diffraction, and scattering effects.

Therefore, to gain a deeper insight into the physics of the propagation mechanisms, intensive MIMO measurement campaigns have been realized in indoor environments to accurately assess the time and angular spread of the specular multipath components (SC) resulting from successive reflection and diffraction effects. To this end, high-resolution parameter estimation techniques have been jointly employed to retrieve the parameters from the measured multi-link channels [2]. Nevertheless, all of the techniques widely disseminated in the community such as ESPRIT, SAGE, or MUSIC have yet failed to include in their data model the presence of time-delay and/or angular diffuse multipath

components (DMC) resulting from scattering, which can be particularly rich in indoor scenarios [3]. It follows that, due to the inadequacy of their data models, these algorithms are expected to provide very poor estimates of the SC parameters and could mislead the development of faithful propagation prediction models.

To highlight the impact of the DMC on the SC parameter estimation accuracy and the necessity to include it into data models, the performance of high-resolution parameter estimation algorithms must be evaluated. Evaluating an estimator is typically accomplished by first emulating synthetic multi-link channels from which all SC and DMC parameters are *a-priori* known. The parameters of the complex channel transfer functions are then estimated and compared with the exact ones. Nevertheless, it is critical to understand that the emulated multi-link channels must be as realistic as possible. Hence, the emulating framework ought to be partially or fully based on measured indoor SIMO channels.

In this work, the performance of three state-of-the-art high-resolution parameter estimation algorithms is evaluated from synthetic measurement-based indoor SIMO channels. The two algorithms were chosen upon their ability to treat DMC or not (i.e. include DMC into the data model or not). The first two algorithms ESPRIT [4] and SAGE [5] do not include time-delay and angular DMC in their data model. On the other hand, the third algorithm RiMAX was developed recently to incorporate time-delay DMC [6]. Note that both time-delay and angular DMC were treated in [7] with an approximate maximum likelihood (ML) estimator. In particular, the performance is discussed for various DMC to SC power ratio scenarios that describe the environment ability to scatter low- or high-power radio-waves.

In the following Section, the method to emulate, from actual measurements, synthetic indoor MIMO channels that include DMC is provided to the reader. Sufficient statistics being required to evaluate the performance of both estimators,

the approach is described in the Simulations Section. Before concluding, the performance of both estimators for all presented scenarios is discussed in the Results Section.

II. RADIO CHANNEL DATA MODEL

The static sampled radio channel investigated in this work $\mathbf{h}(\mathbf{f}, \boldsymbol{\theta})$ has the MIMO double directional structure of a multipath channel [8] given by the superposition of the coherent steering vector $\mathbf{s}(\theta_{sp})$ and DMC \mathbf{d}_{dmc} [6]. DMC being understood as a multivariate circular normal process with zero mean, \mathbf{h} can be defined as:

$$\mathbf{h} = \mathbf{s}(\boldsymbol{\theta}_{sp}) + \mathbf{d}_{dmc} \sim N_c(\mathbf{s}(\boldsymbol{\theta}_{sp}), \mathbf{R}(\boldsymbol{\theta}_{dmc})) \quad (1),$$

where the full correlation matrix of a narrow-band Kronecker-separable channel has the following structure:

$$\mathbf{R}(\boldsymbol{\theta}_{dmc}) = \mathbf{R}_{M_R} \otimes \mathbf{R}_{M_T} \otimes \mathbf{R}_f(\boldsymbol{\theta}_{dmc}) \quad (2).$$

\mathbf{R}_{M_R} and \mathbf{R}_{M_T} describe the angular distribution of the DMC and are here treated as identity matrices to eliminate this component. Note that this aspect has been treated in [7] and related works. On the other hand, $\mathbf{R}_f(\boldsymbol{\theta}_{dmc})$ describes the DMC time-delay distribution. $\mathbf{R}_f(\boldsymbol{\theta}_{dmc})$ has a Toeplitz structure and includes additive white Gaussian noise (AWGN) from the measurement equipment. Regardless of the DMC physical mechanism (either angular or time-delay), it can be regarded as a corrupting coloured noise which is not accounted for in standard data models. Indeed, one typically considers AWGN channels with covariance matrix $\sigma^2 \mathbf{I}$.

Here, for the sake of simplicity, the propagation path parameters θ_{sp} were generated by an in-house 2D ray-tracing in an empty 66 m x 32 m x 10.8 m room. This room models an existing sports center located on the University of Lille Campus. In this work, θ_{sp} denote the set of parameters time-delay of arrival (TDOA), and direction of arrival/departure (DOA/DOD). The deterministic steering vector $\mathbf{s}(\theta_{sp})$ is constructed following:

$$\mathbf{s}(\theta_{sp}) = \mathbf{B}(\boldsymbol{\mu}) \cdot \gamma \quad (3),$$

where the matrix valued function $\mathbf{B}(\boldsymbol{\mu})$ is a concatenated description of the radio channel (time-delay, temporal, angular and frequency response of transmitter/receiver) and γ the linear path weight, respectively. The typical exponential model is employed to form $\mathbf{B}(\boldsymbol{\mu})$ where $\boldsymbol{\mu}$ is the normalized parameter (TDOA, DOA, and DOD). Hence, given the studied problem, a three-dimensional (3D) estimator must be deployed.

The distributed diffuse scattering parameters θ_{dmc} were retrieved from static SIMO measurements in the sports center [9]. θ_{dmc} consist in a set of four parameters α_0 , α_1 , β_d , and τ_d ; variance of the circular (i.i.d.) normal distributed noise, DMC peak power, coherence bandwidth normalized to the measurement bandwidth, and base TDOA normalized to the total length of the observed impulse response, respectively [6]. The time-delay covariance matrix is given by:

$$\mathbf{R}_f(\boldsymbol{\theta}_{dmc}) = \text{toep}(\boldsymbol{\kappa}(\boldsymbol{\theta}_{dmc}), \boldsymbol{\kappa}(\boldsymbol{\theta}_{dmc})^H) \quad (4),$$

where toep is the Toeplitz operator. $\boldsymbol{\kappa}(\boldsymbol{\theta}_{dmc})$ is the sampled version of the power spectrum density constructed as:

$$\boldsymbol{\kappa}(\boldsymbol{\theta}_{dmc}) = \frac{\alpha_1}{M_f} \left[\frac{1}{\beta_d} \frac{e^{-j2\pi\tau_d}}{\beta_d + j2\pi \frac{1}{M_f}} \cdots \frac{e^{-j2\pi(M_f-1)\tau_d}}{\beta_d + j2\pi \frac{M_f-1}{M_f}} \right]^T + \alpha_0 \mathbf{e}_0 \quad (5),$$

where $\mathbf{e}_0 = [1 \ 0 \ 0 \cdots 0]^T$ is a unit vector.

III. SYNTHETIC CHANNELS & SIMULATIONS

A single SISO link is constructed as follows: steering vectors $\mathbf{s}(\theta_{sp})$ are generated for a random Rx and Tx position; the reflection order for those paths varying between 0 (for the LOS path) and 6. 50 propagation paths were selected to construct a single SISO link but depending upon the geometrical configuration, only 10 to 20 paths were shown to have an SNR sufficiently large to be detected by the estimators as shown in Figs. 1 and 2.

The SIMO measurements reported in [9] were then used to extract the DMC parameters. Those parameters characterize the scattering properties of the considered indoor scenario. The SC power was then set as the SC to DMC power ratio P_{SC}/P_{dmc} with

$$P_{dmc} = \frac{\alpha_1}{\beta_d} e^{\beta_d \tau_d} + \alpha_0 \quad (6),$$

where α_0 is the measurement noise power. Note that this is equivalent to defining a Signal to Colored Noise Ratio (SCNR). Three power ratio scenarios are investigated in this work: $P_{SC}/P_{dmc} = 0.7/0.3$ (30% DMC), $P_{SC}/P_{dmc} = 0.5/0.5$ (50% DMC), and $P_{SC}/P_{dmc} = 0.3/0.7$ (70% DMC). Those three scenarios were chosen as to adequately assess the estimation performance in the presence of strong or weak DMC [10].

The complete synthetic multi-link channel is finally reconstructed into a virtual 16 x 16 MIMO link with 4 x 4 uniform rectangular arrays (URAs) for both Tx and Rx, respectively. Omni-directional antennas are chosen for the arrays to ensure uniform gain across the angular domain. \mathbf{h} was generated at 3.5 GHz over a 40 MHz bandwidth and 1 MHz frequency step. 25 channel realizations were emulated for each scenario with 10 independently and identically distributed (i.i.d.) observations per link to statistically assess the performance of the estimators.

Figure 1 presents an arbitrary emulated power delay profile which has been subsequently estimated by RiMAX. In this example, 9 propagation paths are correctly detected by the algorithm. A set of 4 paths with low SNR could not be detected by the algorithm. The blue curve is the synthetic PDP constructed as the superposition of the specular and diffuse components (red curve) over the 40 MHz bandwidth. In addition to the TDOA estimation, Fig. 2 presents the exact DOA and DOD parameters and their estimates. Again, a good agreement is found.

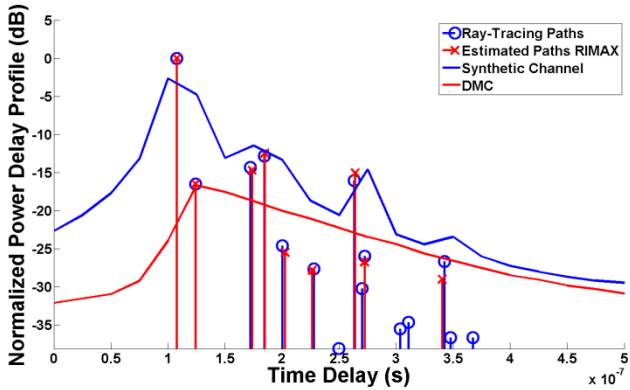


Fig. 1 Arbitrary normalized synthetic Power Delay Profile (in dB) and DMC over a 40 MHz bandwidth. The exact (blue circle) and estimated (red cross) propagation paths are shown over an infinite bandwidth.

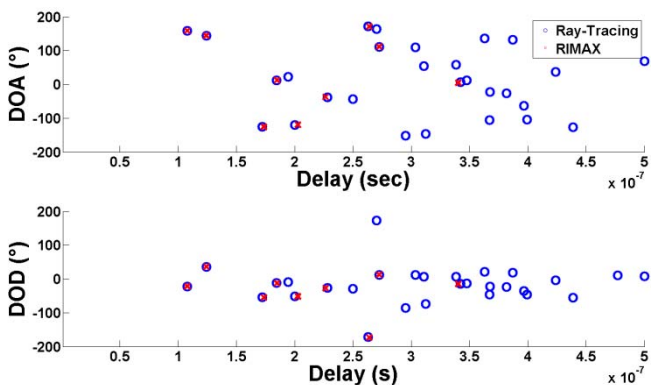


Fig. 2 Exact (blue circle) vs. estimated (red cross) angular parameters extracted from the synthetic channel shown in Fig. 1.

IV. RESULTS & DISCUSSION

For each power ratio scenario, ESPRIT, SAGE and RiMAX were used to extract around 240 SCs from the constructed radio channels \mathbf{h} . It is noteworthy that the number of signals estimated by RiMAX was fed as an input to ESPRIT and SAGE to perform fair statistics. The estimated parameters were paired with their true counterpart with the multipath component distance (MCD) algorithm [11]. Then, the absolute estimation error was computed between the estimates and true values.

In Fig. 3, the empirical cumulative distribution function (ECDF) of the absolute estimation error is shown for the SC DOA parameter for all three algorithms. The black (solid) curves correspond to $P_{SC}/P_{dmc} = 0.3/0.7$, blue curves (dash) to $P_{SC}/P_{dmc} = 0.7/0.3$, and red curves (dash-point) to $P_{SC}/P_{dmc} = 0.5/0.5$. For each power ratio scenario, the DOA estimation error values computed from ESPRIT and SAGE estimates are observed to be larger. In addition, the errors are spread in comparison to those obtained from RiMAX estimates. This poor estimation accuracy of ESPRIT and SAGE is expected as the presence of DMC will strongly corrupt the algorithms' ability to separate the signal subspace from the noise subspace. This inadequacy to separate the signal subspace from the

noise subspace arises from the fact that the covariance matrix is non-diagonal due to the DMC presence. Nevertheless, it is observed that ESPRIT is less sensitive to the DMC presence than SAGE. Nevertheless, both algorithms show some dependence to the DMC power.

Meanwhile in Fig. 3, RiMAX is able to accurately estimate more than 80% of the SC DOAs with errors close to 1° without any dependence to the DMC power. It can be concluded that RiMAX clearly improves SC DOA estimates over ESPRIT and SAGE in the presence of DMC. For RiMAX, a mean DOA root mean square (rms) estimation error of 0.76° is computed from all scenarios with 0.95 confidence level. The same conclusion could be drawn for the estimation of the SC DOD parameter.

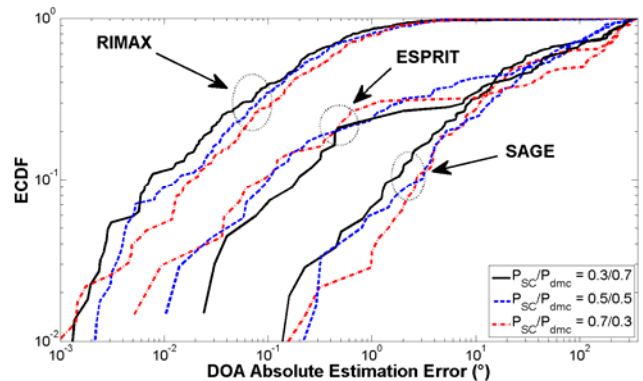


Fig. 3 SC DOA absolute estimation error computed with ESPRIT, SAGE, and RiMAX for the three power ratio scenarios $P_{SC}/P_{dmc} = 0.3/0.7$ (solid black), $P_{SC}/P_{dmc} = 0.7/0.3$ (blue dashes), and $P_{SC}/P_{dmc} = 0.5/0.5$ (red point-dashes).

Figure 4 shows the ECDF of the absolute estimation errors for the SC TDOA. Similar conclusions as for the SC DOA parameter can be drawn: RiMAX reduces the TDOA estimation errors to about 1 for more than 70% of estimated SC TDOA (1 ns absolute error) whereas large estimation errors are obtained with ESPRIT and SAGE. For RiMAX, a mean TDOA RMS estimation error of 1.02 ns is computed from all scenarios with 0.95 confidence level. Although ESPRIT and SAGE provide poor TDOA estimates, the former performs much better than SAGE but shows a higher degree of dependency to the DMC.

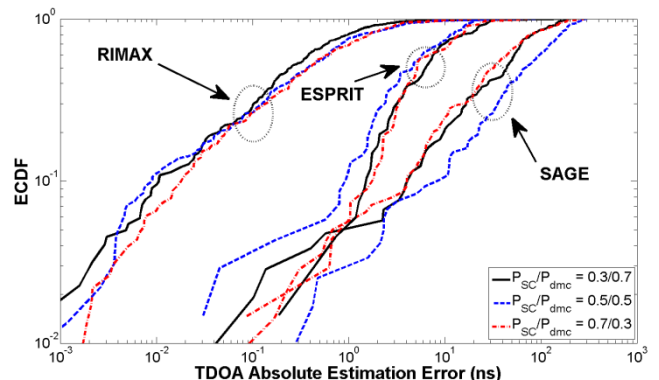


Fig. 4 SC TDOA absolute estimation error computed with ESPRIT, SAGE, and RiMAX for the three power ratio scenarios $P_{SC}/P_{dmc} = 0.3/0.7$ (solid

black), $P_{SC}/P_{dmc} = 0.7/0.3$ (blue dashes), and $P_{SC}/P_{dmc} = 0.5/0.5$ (red point-dashes).

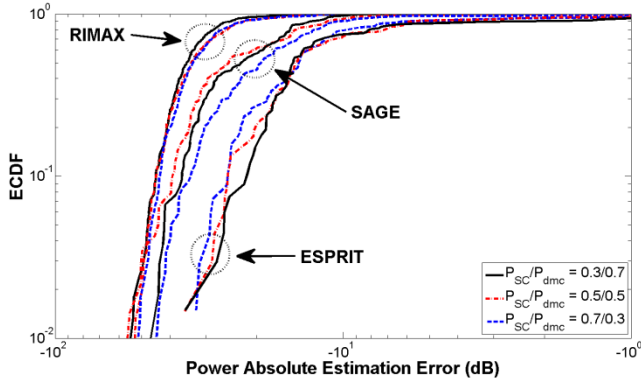


Fig. 5 SC Power absolute estimation error computed with ESPRIT, SAGE, and RiMAX for the three power ratio scenarios $P_{SC}/P_{dmc} = 0.3/0.7$ (solid black), $P_{SC}/P_{dmc} = 0.7/0.3$ (blue dashes), and $P_{SC}/P_{dmc} = 0.5/0.5$ (red point-dashes).

Finally, Fig. 5 shows the ECDF of the absolute estimation errors for the SC Power. RiMAX reduces the power absolute errors to about -20 dB for more than 90% of estimates whereas larger RMS errors are obtained with ESPRIT (0 dB) and SAGE (-10 dB). For RiMAX, a mean power rms estimation error of -26.35 dB is computed from all scenarios with 0.95 confidence level. In contrast to the non-linear TDOA, DOA and DOD parameters, SAGE provides a better estimation for the power parameter but shows a higher degree of dependency to the DMC.

CONCLUSION

The high-resolution parameter estimation algorithms ESPRIT, SAGE and RiMAX were applied onto synthetic MIMO radio channels in the presence of measurement-based DMC. Our results strongly demonstrate that RiMAX outperforms ESPRIT and SAGE for all simulated scenarios. The poor SC parameters estimation performance is here attributed to the absence of DMC in the ESPRIT and SAGE data model. In addition, ESPRIT and SAGE are observed to be strongly dependent to the DMC power thus resulting in larger error spread. This study highlights the fact that DMC must be taken into consideration when channel estimation techniques are employed. Adding DMC in the data model of estimators is therefore critical to the development of faithful propagation models and should be further investigated.

Future research on this topic will focus, for a given configuration, on the optimal settings (such as the number of

searched SC paths) for the RiMAX algorithm to estimate a higher percentage of SC paths correctly with negligible error. In any cases, a better understanding of the diffusion mechanism may also be gained by investigating this phenomenon in various environments. This would not only lead to improved mathematical descriptions but also to the development of more accurate high-resolution parameters estimation algorithms.

ACKNOWLEDGMENT

This work has been carried out in the framework of the CISIT (Campus International sur la Sécurité et l'Intermodalité Transports) project and funded by the French Ministry of Research, the Region Nord Pas de Calais and the European Commission (FEDER funds). Wout Joseph is a Post-Doctoral Fellow of the FWO-V (Research Foundation - Flanders).

REFERENCES

- [1] G. J. Foschini, M. J. Gans, "On limits of wireless communications in a fading environment", *Wireless Personal Communications*, vol. 6, pp. 311-335, 1998.
- [2] R. S. Thoma, D. Hampicke, M. Landmann, A. Richter and G. Sommerkorn, "Measurement-based channel modelling," *ICEAA 2003*, Torino, Sept. 2003.
- [3] J. Poutanen, K. Haneda, J. Salmi, V.-M. Kolmonen, and P. Vainikainen, "Angular characteristics of dense multipath components in indoor radio channels", 9th COST2100 MCM meeting, TD(09)911, Vienna, Austria, September 28-30 2009.
- [4] R. Roy, T. Kailath - "ESPRIT: estimation of signal parameters via rotational invariance techniques", *IEEE Transactions on Acoustics and Speech Signal Processing*, vol. 37, pp. 984-995, 1989.
- [5] A. Richter, "Estimation of radio channel parameters: models and algorithms", Thesis, TU Ilmenau, 2005.
- [6] J. A. Fessler, A. O. Hero, "Space-alternating generalized expectation-maximization algorithm," *IEEE Transactions on Signal Processing*, vol. 42, no.10, pp.2664-2677, October 1994.
- [7] C. B. Ribeiro, A. Richter, and V. Koivunen, "Joint Angular and Delay Domain MIMO Propagation Parameter Estimation Using an Approximate ML Method," *IEEE Transactions on Signal Processing*, vol. 55, no. 10, pp. 4775-4790, October 2007.
- [8] M. Steinbauer, A. Molisch, and E. Bonek, "The doubledirectional mobile radio channel," *IEEE Antennas and Propagation Magazine*, vol. 43, no. 4, pp. 51-63, Aug. 2001.
- [9] E. Tanghe, W. Joseph, M. Lienard, A. Nasr, P. Stefanut, D. P. Gaillot, P. Degauque, and L. Martens, "Clustering of channel parameters by block diagonal matrix decomposition", 7th COST2100 MCM meeting, TD(09)712, February 16-18 2009, Braunschweig, Germany.
- [10] J. Salmi, J. Poutanen, K. Haneda, A. Richter, V.-M. Kolmonen, P. Vainikainen, A. Molisch, "Incorporating Diffuse Scattering in Geometry-based Stochastic MIMO Channel models", 10th COST2100 MCM meeting, TD(10)10047, February 3-5 2010, Athens, Greece.
- [11] M. Steinbauer, H. Özcelik, H. Hofstetter, C. F. Mecklenbräuker, and E. Bonek, "How to quantify multipath separation," *IEICE Trans. Commun.*, vol. E85-C, no. 3, pp. 552-557, Mar. 2002.